

Preparation of Uniformly Dispersed N-isopropylacrylamide/Acrylic acid/Nanosilver Composite Hydrogel and its Anti-Mold Properties

Rui Peng,^a Huilong Yu,^b Chungui Du,^{a,*} Jingjing Zhang,^a Ailian Hu,^a Qi Li,^a Yating Hua,^a Hongzhi Liu,^a and Shimin Chu^a

To overcome the agglomeration tendency of nanosilver composite hydrogels and to improve their anti-mold properties, a method of preparing N-isopropylacrylamide/acrylic acid/nanosilver composite hydrogel was developed using the free radical polymerization method. The composite hydrogel was characterized *via* infrared spectroscopy, dynamic light scattering, transmission electron microscopy, and X-ray photoelectron spectroscopy in order to explore the effects of the acrylic acid content on particle size and dispersion properties of the composite hydrogels. The elemental composition, microstructure, and anti-mold properties of the bamboo strips treated with the composite hydrogel were also determined. The results showed that the composite hydrogel prepared using the novel method described in this study had good dispersity. Composite hydrogels with the smallest particle size and optimized dispersion were produced when AAc concentration was 0.64 $\mu\text{L/mL}$. The composite hydrogel effectively filled and covered the bamboo cells after treatment. Moreover, it displayed good anti-mold properties as well as retaining the color of the bamboo.

Keywords: N-isopropylacrylamide (NIPAm); Acrylic acid (AAc); Nanosilver (AgNPs); Composite hydrogel; Dispersity; Bamboo strips; Anti-mold properties

Contact information: a: School of Engineering, Zhejiang A & F University, Hangzhou, Zhejiang 311300 China; b: National Furniture Product Quality Supervision and Inspection Center, Ganzhou, Jiangxi 341400 China; *Corresponding author: chunguidu@163.com

INTRODUCTION

As a new renewable resource with a short growth cycle and a high economic value, bamboo has been widely used in interior decoration, architecture, automobile manufacturing, and other fields (Chung and Yu 2002; Sharma *et al.* 2015; Yuan *et al.* 2017; Liu *et al.* 2019; Wu *et al.* 2019; Liu *et al.* 2020). However, bamboo is vulnerable to mold invasion, and the resulting loss accounts for approximately 10% of the total bamboo output (Zhang *et al.* 2020). Therefore, it is of great importance to study the mold prevention of bamboo. The author's team used N-isopropyl acrylamide (NIPAm) as a monomer to synthesize a thermo-sensitive silver-borne nano-hydrogel, which was applied in order to mildew-proof bamboo material, which achieved good mildew-proofing effects (Yu *et al.* 2017). However, the authors found that the addition of nanosilver (AgNPs) in the composite hydrogel would cause a small amount of precipitation, agglomeration, or oxidation over time, which resulted in reduced antibacterial properties. In addition, the oxidized AgNPs would turn the bamboo black during the mold-proofing process, thus affecting the beauty of the bamboo.

Dispersion protectants are often used to overcome the shortcomings of AgNPs, *e.g.*, precipitation, agglomeration, *etc.* (Eghbalifam *et al.* 2015; Ge *et al.* 2017; Gao *et al.* 2018; Qi *et al.* 2018; Zhou *et al.* 2019). The dispersion protectants and the AgNPs particles undergo chemical or physical adsorption, and a molecular protection layer will form on the particle surfaces, preventing the aggregation of AgNPs particles. Polyvinyl pyrrolidone (PVP) is a non-ionic surfactant with good solubility, high polymer surface activity, complexability, as well as other desirable properties (Begum *et al.* 2016; Gilcrease *et al.* 2020; Hu *et al.* 2020). It is commonly used as a dispersive protective agent for AgNPs (He *et al.* 2017a,b). However, the addition of a single PVP does not provide major dispersion effects for AgNPs, so the concentration of AgNPs must be increased, which will lead to the tedious removal process of the subsequent surfactants. A large number of studies have found that combinations of dispersing protectants used together with the polymer monomers can produce better dispersing stability effects than a single dispersing agent. Acrylic acid (AAc) is a hydrophilic monomer containing carboxyl groups, which have strong complexation to Ag^+ (Hu *et al.* 2014). Therefore, with NIPAm and AAc as the hydrogel matrix and PVP as the protective agent, the authors prepared a novel composite hydrogel *via* the free radical polymerization method (Wei *et al.* 2016, 2018; Huang *et al.* 2019), and evaluated the addition amount of AAc in terms of the composite hydrogel particle size, dispersion performance, and bamboo anti-mold properties. This preparation method has good anti-mold properties due to the addition of NIPAm/AgNPs and should provide a theoretical reference compound for antibacterial hydrogel production.

EXPERIMENTAL

Materials

The *N*-Isopropyl acrylamide (NIPAm AR) was purchased from TCI Chemicals Co., Ltd. (Tokyo, Japan). The acrylic acid (AAc), *N,N'*-methylenebisacrylamide (MBA), tetramethylethylenediamine (TMEDA), potassium persulfate (KPS), silver nitrate (AgNO_3), sodium borohydride (NaBH_4), and polyvinylpyrrolidone (PVP) were all supplied by Aladdin Reagent Co., Ltd. (Pico Rivera, CA). The deionized water was prepared in the laboratory.

The bamboo strips were purchased from the Zhejiang Yongyu Bamboo Industry Co., and the purchased Moso bamboo was processed into strips with the dimensions of 50 mm \times 20 mm \times 5 mm (length \times width \times thickness) so that no node was formed and a 10% moisture content was maintained.

Methods

Preparation of the composite hydrogels

A 250 mL 3-neck round bottom flask containing 100 mL of deionized water was purged with high purity N_2 at room temperature while stirring until the flask was completely free of oxygen. Different concentrations of AAc were prepared in the flasks (AAc concentrations were 0, 0.16, 0.32, 0.48, 0.64, and 0.80 $\mu\text{L}/\text{mL}$, respectively). This was followed by the addition of 0.682 g of NIPAm monomer, 0.1 g of PVP protectant, 1700 μL of MBA crosslinker (0.015 g/mL, prepared in the lab), and 93 μL of TEMED catalyst. The solution was properly mixed and kept in the dark. Under a N_2 atmosphere, 600 μL of AgNO_3 solution (1.0 M, prepared in the lab) was slowly added and stirred for

1 h, followed by the addition of 1000 μL of KPS initiator (0.030 g/mL). The mixture was allowed to polymerize for 6 h under a N_2 atmosphere, resulting in a clear and transparent nano-hydrogel solution. Afterwards, 1200 μL of NaBH_4 solution (1.0 M) was added, and the solution was kept in the dark for 12 h. Finally, the reaction mixture was purified with a dialysis bag (MWCO: 8000 to 14000) to remove any unreacted monomers, and the different types of composite hydrogels (P0, P16, P32, P48, P64, and P80) were obtained and stored at room temperature for use. Figure 1 shows the preparation of the composite hydrogels.

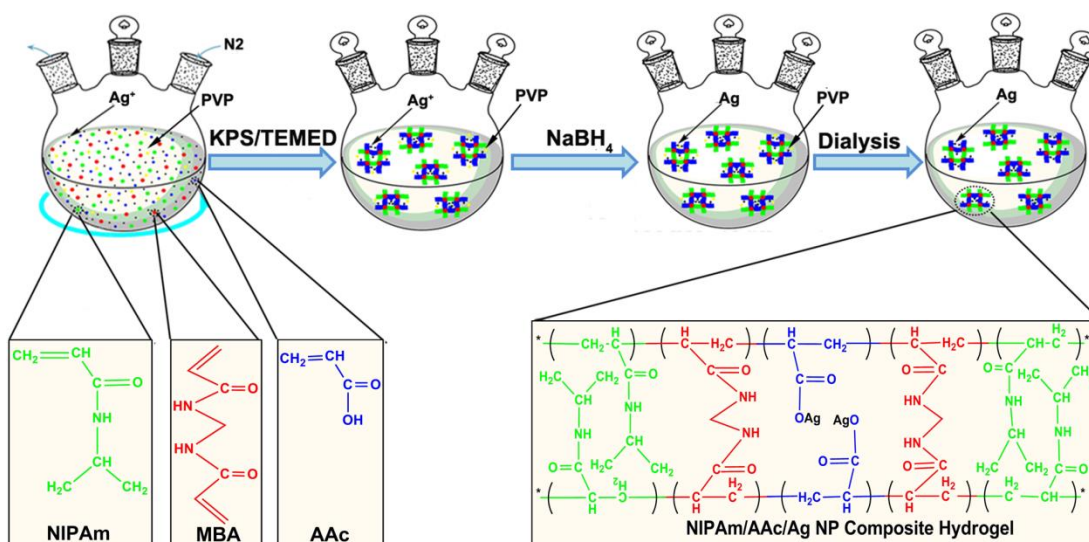


Fig. 1. Schematic diagram of the preparation of the composite hydrogels

Infrared spectroscopic (FT-IR) analysis

The lyophilized composite hydrogel samples were ground into a powder and mixed with potassium bromide at a mass ratio of 1 to 100 and pressed into thin films. Its molecular structure was analyzed *via* Fourier-transform infrared spectroscopy (FT-IR) (IRPrestige-21 spectrometer) with a resolution of 4 cm^{-1} and a scanning range from 4000 cm^{-1} to 400 cm^{-1} . Each sample was scanned in triplicate, and the spectra were required to match at least twice.

Dynamic light scattering (DLS) analysis

A few drops of the composite hydrogel solution were added into a quartz cell and diluted. Bubbles in the solution were removed by shaking, and the particle size of the composite hydrogel was analyzed *via* a DLS instrument (ZetaPALS-31484). The measurement conditions were as follows: a laser emission of 658 nm, a laser energy of 4.0 mW, a background scattering of 173° , and temperature of 25°C . Each sample was scanned five times, and the results were averaged.

Transmission electron microscopy (TEM) analysis

A drop of the composite hydrogel solution was diluted three times and mixed with a drop of 2.0 wt.% uranyl acetate solution. It was then placed on a copper mesh covered with carbon film, and the excess liquid was absorbed with clean filter paper after approximately 4 min. After the mesh naturally dried, the composite hydrogel was scanned *via* a TEM (JEOL JEM-1200) instrument working at an accelerating voltage of

80 kV to observe the microstructure of the composite hydrogel.

Impregnation of the bamboo strips with the composite hydrogel

The bamboo strips were treated with boiling water for 2 h, followed by 1.0 wt.% NaOH solution for 2 h, deionized water for 2 h, 1.0 wt% HCl for 2 h, and finally dried to a moisture content of approximately 10.0%. The treated strips were then immersed in the composite hydrogel solution for 1.5 h at room temperature and a pressure of 0.5 MPa before removing for use.

X-ray photoelectron spectrometric (XPS) analysis of the treated bamboo strips

After treatment with the composite hydrogels, the bamboo strips were sliced, and the surface elemental composition of the slices was analyzed via XPS (ESCALAB 250Xi). The analysis conditions were as follows: the radiation type was Al K α , the power was 350 W, and the pressure was 10⁻⁹ Torr.

Scanning electron microscopic (SEM) analysis of the treated bamboo

The treated bamboo slices were further analyzed via SEM (Hitachi TM 1000) to observe the cross-sectional microscopic structures. After fixing conductive glue on the sample station, the sample was coated with gold for 60 s with an acceleration voltage of 5.0 kV.

Anti-mold properties of treated bamboo strips

The anti-mold properties of the bamboo strips treated with the composite hydrogels were tested according to the GB/T standard 18261 (2013). The strain suspensions of *Penicillium citrinum* (PC), *Trichoderma viride* (TV), *Aspergillus niger* (AN), and mixed molds (PC, TV, and AN in a 1 to 1 to 1 ratio, abbreviated as PTA) were spread evenly on a Petri dish containing the plate medium and put in sterilized U-shaped solid glass rods. Afterwards, the dish containing the molds was cultured in an incubator at a temperature of 28 °C \pm 2 °C and a relative humidity of 85% \pm 5%. After successfully culturing the mold, the bamboo was placed on the U-shaped glass rods, and the edges of the Petri dish were sealed with a sealing film. Finally, the bamboo strips were placed in a Petri dish in the incubator for anti-mold testing.

Table 1. Classification Standard of Surface Infection Levels of Samples

Infection Levels	Infected Area of Sample
0	No hyphae or mildew on the sample surface
1	Infected area of sample < 1/4
2	Infected area of sample 1/4–1/2
3	Infected area of sample 1/2–3/4
4	Infected area of sample > 3/4

During the test, the bamboo strips in the incubator were observed and recorded for mold infection every alternate day. After 28 d, the bamboo samples were photographed, the area of the bamboo strips infected by the fungus were observed and analyzed to determine the infection levels of the bamboo strips (Table 1) (Zhang *et al.* 2020), each group was repeated three times and the results were averaged. Finally, in order to analyze

the anti-mold performance of the NIPAm/AAc/Ag NPs composite hydrogels, the authors compared the anti-mold results of the composite hydrogels with the results of the silver-loaded thermo-sensitive nanogels (Yu *et al.* 2017), and paid attention to the color change of bamboo material after the anti-mold testing procedure.

RESULTS AND DISCUSSION

Fourier-Transform Infrared Spectroscopy (FT-IR) Analysis of the Composite Hydrogels

Figure 2 shows the FT-IR spectra of the different types of composite hydrogels prepared by adding different amounts of AAc. The characteristic stretch vibrational absorption peak at 1620 cm^{-1} for the C=C conjugation as well as the out-of-plane deformation vibrational peak at 990 cm^{-1} for the terminal alkene hydrogen atoms in the NIPAm spectra disappeared in the spectra of the different types of composite hydrogels. This indicated the successful polymerization of NIPAm, forming PNIPAm hydrogels.

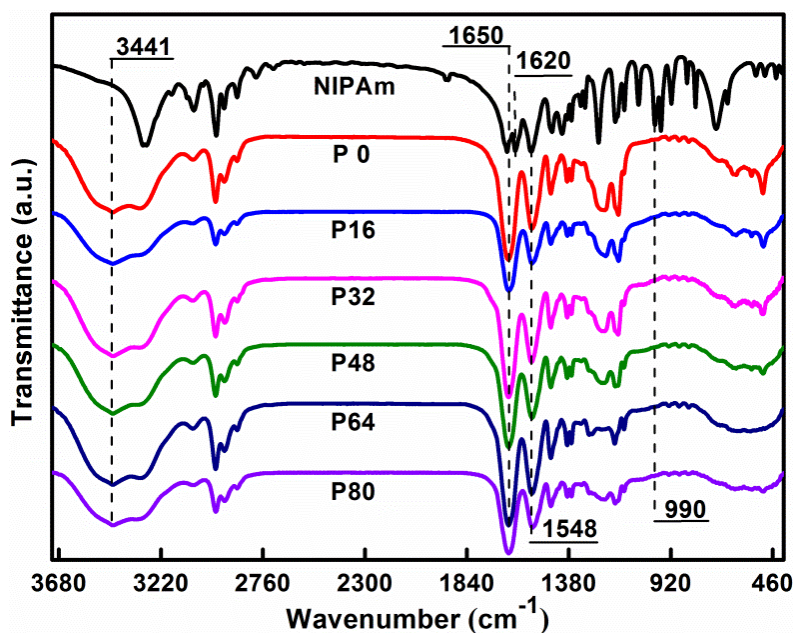


Fig. 2. FT-IR spectra of the composite hydrogels

In spectra of hydrogel samples P0 to P80, there was a wide absorption band at 3441 cm^{-1} , which was the stretching vibration peak of -OH and the result of water adsorption *via* PVP molecules. The peak at 1650 cm^{-1} was a stretching vibration peak of the C=O of the amide group, while the peak at 1548 cm^{-1} was a variable angle vibration peak caused by the stretching vibration of the N-H and C-N bonds. The carboxyl group in the AAc formed hydrogen bonds with Ag^+ (Meng *et al.* 2016; Hong *et al.* 2017); however, it weakened the hydrogen bonding force between the amide groups in PNIPAm and Ag^+ (Devaki *et al.* 2014; Ma *et al.* 2019). Thus, the absorption bands of these functional groups in the composite hydrogels were only slightly altered when AAc was added. The change was minor, and the original molecular structure was mostly maintained (Guo *et al.* 2014; Wang *et al.* 2016).

Dynamic Light Scattering (DLS) Analysis of the Composite Hydrogels

A dynamic light scattering particle size (DLS) instrument was used to measure the particle size distribution of the different types of composite hydrogels and the effects of the addition of AAc on particle size. The results are shown in Fig. 3.

Figure 3a demonstrated that the particle size of the different types of composite hydrogels ranged from 25 nm to 343 nm and showed a regular Gaussian distribution pattern. Figure 3b indicates that the particle sizes of the composite hydrogels were greatly influenced by the concentration of AAc. When the concentration of AAc ranged from 0 to 64 $\mu\text{L}/\text{mL}$, the particle size rapidly decreased as the concentration of AAc increased. In contrast, when the concentration of AAc ranged from 0.64 $\mu\text{L}/\text{mL}$ to 0.80 $\mu\text{L}/\text{mL}$, the particle size of the composite hydrogel rapidly increased as the concentration of AAc increased. When no AAc was added, the composite hydrogel displayed the largest particle size (147.0 nm). When the concentration of AAc was 0.64 $\mu\text{L}/\text{mL}$, the composite hydrogel had the smallest particle size (59.4 nm). Thus, 0.64 $\mu\text{L}/\text{mL}$ of AAc was the turning point in the particle size of the synthetic composite hydrogel. This was also the optimal concentration of AAc for preparation of the composite hydrogel.

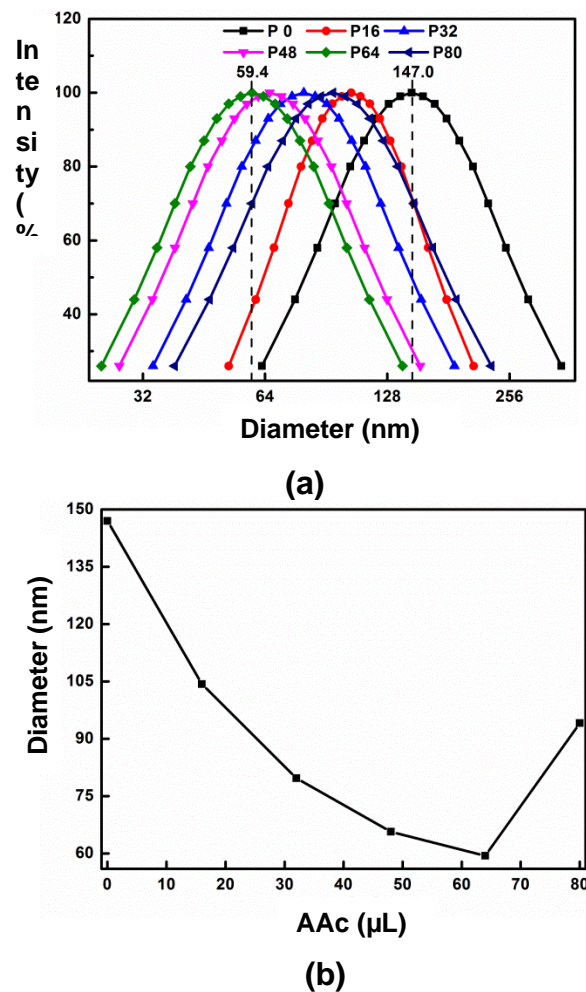


Fig. 3. The particle size distribution of the composite hydrogels and the effect of AAc on particle size: (a) Size distribution curves; and (b) Effects of the amount of AAc on particle size

The rationale was that when the concentration of AAc was in the range 0 to 0.64 $\mu\text{L}/\text{mL}$, the carboxyl group on AAc formed a strong ionic attraction with the amide group on the PNIPAm chains. The strength of this ionic attraction was stronger than the original hydrogen bond formed between the amide groups and the water molecules. This weakened the hydrophilic effect of the molecular chain of the PNIPAm hydrogel. Meanwhile, the carboxyl groups weakened the binding ability between the amide group and Ag^+ , which led to an overall reduced particle size of the composite hydrogel. When the concentration of AAc ranged from 0.64 $\mu\text{L}/\text{mL}$ to 0.80 $\mu\text{L}/\text{mL}$, the extra AAc attached to the molecular chains of PNIPAm due to the formation of ionic attraction between the AAc and the PNIPAm. The continued addition of AAc further increased the number of carboxyl groups in the hydrogel system, along with the formation of additional hydrogen bonds with water, therefore increasing the hydrogel particle size. Moreover, the adsorption of the Ag^+ ions by $-\text{COOH}$ groups in AAc was another important factor contributing to the increase in the particle size (He *et al.* 2017a,b).

Transmission Electron Microscopy (TEM) Analysis of the Composite Hydrogels

All types of composite hydrogels displayed a uniformly dispersed state. However, it was unclear whether the AgNPs in the composite hydrogels were also uniformly dispersed. For this reason, the microscopic morphology of the different types of composite hydrogels was tested *via* transmission electron microscopy (TEM), and the results are shown in Fig. 4.

Due to the scattering effect of the Ag nuclei on the electron rays, Ag appeared black on the TEM image. In the TEM images of the P0 to P80 samples (scale bar = 500 nm), the composite hydrogel showed an obvious reticular structure, and the dispersion of the AgNPs was observed without any agglomeration (Wu *et al.* 2010). In the magnified TEM images of the P0 to P80 samples (scale bar = 50 nm), the spherical morphology of the AgNPs was revealed with variable dispersion depending on the composite hydrogel type.

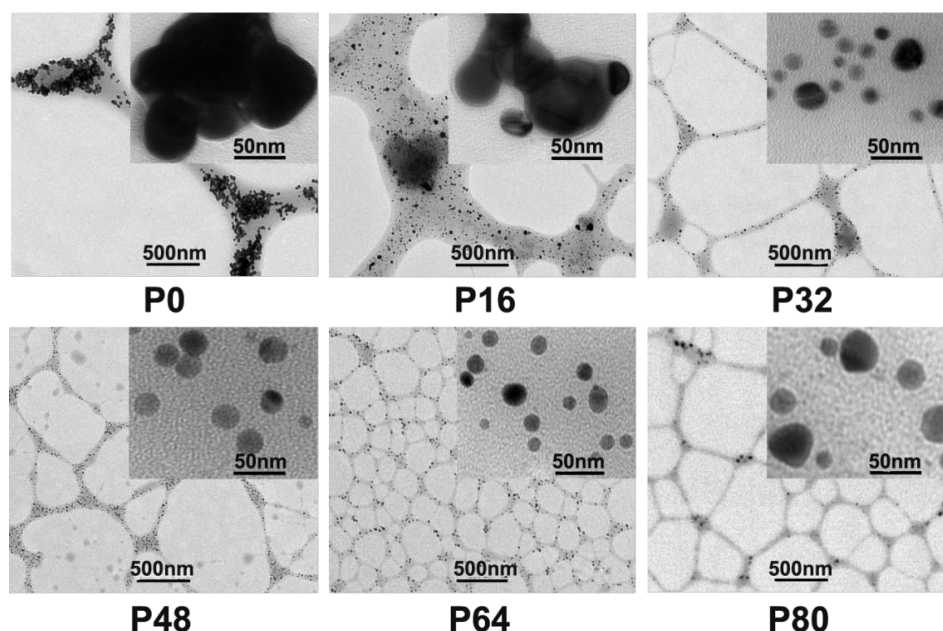


Fig. 4. TEM image of the composite hydrogels

As shown in Fig. 4, the agglomeration and particle size of the AgNPs gradually decreased and became more homogeneously dispersed upon the addition of an increasing concentration of AAc. When the concentration of AAc was 0.64 $\mu\text{L}/\text{mL}$, the AgNPs displayed a homogeneous and optimized dispersion, alongside the formation of the smallest size of composite hydrogels. Further increasing the concentration of AAc deteriorated the dispersion properties of the AgNPs. Additionally, the change in the particle sizes of the composite hydrogels observed from the TEM images showed a dependence on the concentration of AAc. This result was consistent with those obtained from the DLS analysis and further proved the reliability of the experimental results.

X-ray Photoelectron Spectrometric (XPS) Analysis of the Treated Bamboo Strips

The aforementioned results indicated that the optimal concentration of AAc for the free radical polymerization method preparation of composite hydrogels was 0.64 $\mu\text{L}/\text{mL}$. Therefore, the authors prepared and used P64 composite hydrogel to treat the bamboo strips. The strips were further characterized *via* X-ray photoelectron spectroscopy (XPS) to analyze their surface elemental composition. The results are shown in Fig. 5.

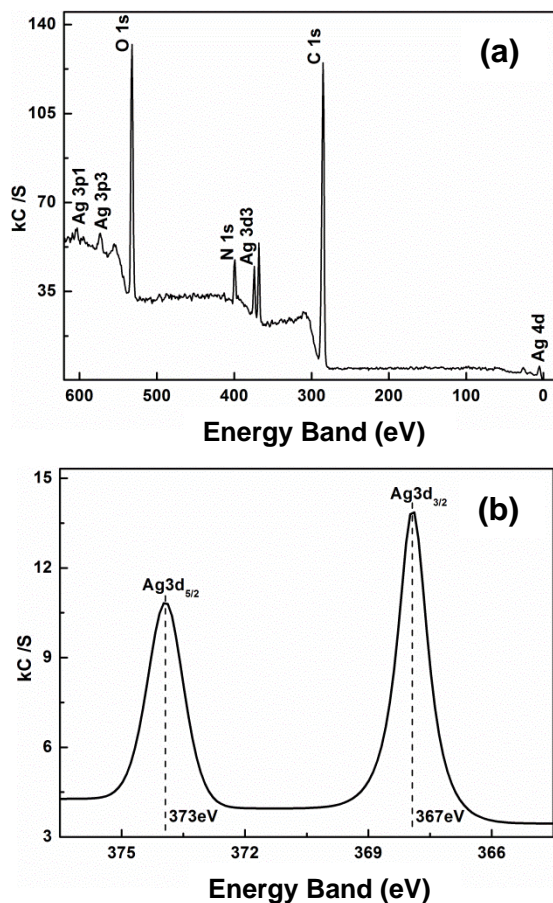


Fig. 5. The XPS spectra of the bamboo strips treated with the composite hydrogel: (a) Full spectrum; and (b) Ag3d spectrum

Figure 5 shows that the full XPS spectrum of the treated bamboo samples (as shown in Fig. 5a) contained not only the characteristic peaks of C, N, and O, but also the characteristic peaks of the Ag element, which indicated that the P64-type composite hydrogel had been successfully loaded onto the bamboo strips. This result was consistent with the results obtained from the elemental composition of the composite hydrogel. Additionally, as shown in Fig. 5a, it was observed that the Ag element showed the characteristic peaks of Ag3p1, Ag3p3, Ag3d3, *etc.* This indicated that the Ag entered into the bamboo strips in multiple forms. In the Ag3d spectra of the treated bamboo samples (as shown in Fig. 5b), the electron binding energies of Ag3d5/2 and Ag3d3/2 were 367.9 eV and 373.9 eV, respectively. These values are extremely close to the standard electron binding energies of 368.2 eV and 374.2 eV of metallic Ag3d3/2 and 3d5/2, respectively. Thus, the electron binding energies of the AgNPs contained in the treated bamboo samples shifted toward lower energies. Because the electron binding energy of the 3d orbital of Ag⁺ was lower than that of Ag, it was inferred that small amounts of Ag⁺ existed, in addition to the large amount of AgNPs in the treated bamboo samples. This was favorable for the antifungal properties of the composite hydrogel because Ag⁺ had a slightly better anti-mold activity than the AgNPs, while maintaining a similar mode of action in the mold cells (Shi and Li 2018), whereas the AgNPs could synergize with the Ag⁺ to exert anti-bacterial effects (Taylor *et al.* 2005).

Scanning Electron Microscopy (SEM) Analysis of the Treated Bamboo Strips

After treatment with the P64 composite hydrogel, the bamboo strips were sectioned in the transverse direction and scanned *via* a scanning electron microscope (SEM) to observe their microstructure. The results are shown in Fig. 6. After treatment with the composite hydrogel, the parenchyma cells, ducts, and other bamboo cells maintained their original microstructural morphology without getting damaged. However, for a small number of parenchyma cells, ducts, and other bamboo cells, the microscopic cross-section became ambiguous, and the boundaries between the cells were not obvious, while some had no boundaries at all. The primary reason for this phenomenon was that after treatment with the composite hydrogel, the cells found within the cell lumen and the cell walls of the bamboo strips were filled or covered with a large number of composite hydrogel and AgNPs particles. Therefore, the impregnation treatment of the bamboo strips with composite hydrogels was beneficial for improving its relevant properties by increasing the loading amount of composite hydrogel.

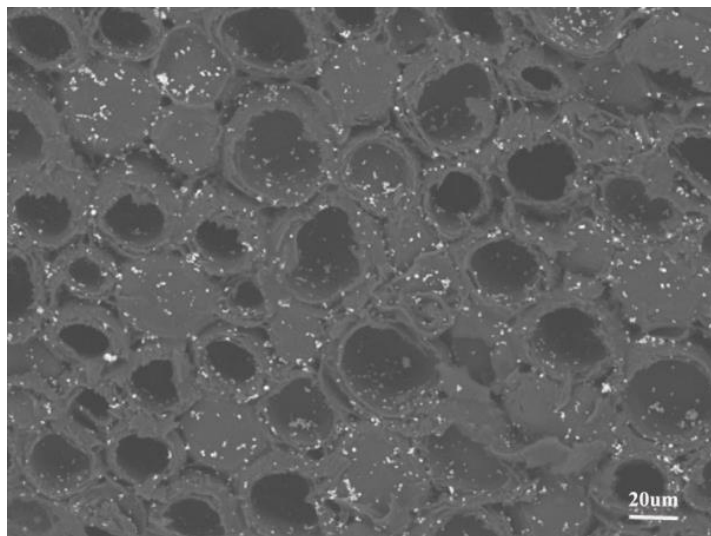
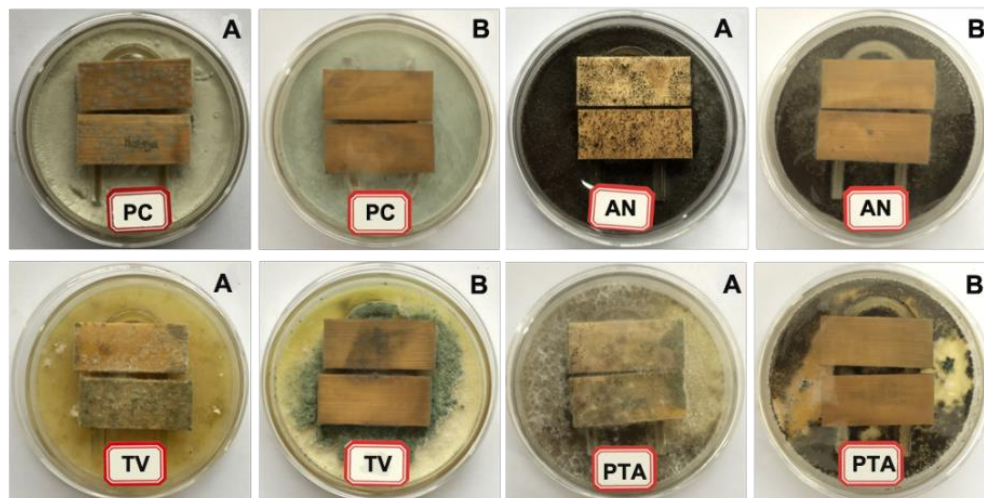


Fig. 6. The SEM image of a bamboo slice treated with the composite hydrogel

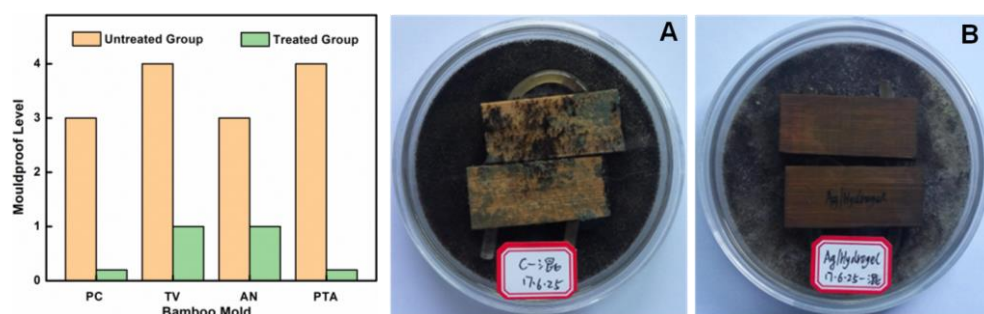
Analysis of the Antifungal Properties of the Treated Bamboo Strips

The anti-mold properties of the bamboo strips treated with the P64 composite hydrogel were determined and compared with that of the untreated bamboo strips within 28 d. The results are shown in Fig. 7.

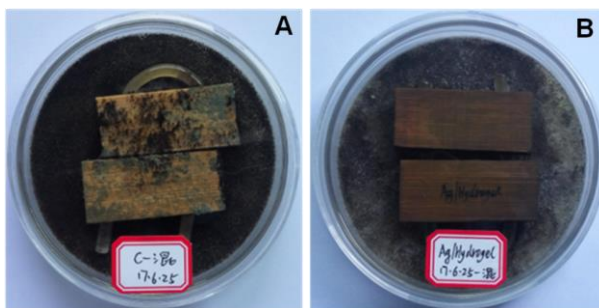
As shown in Fig. 7a and 7c, the bamboo strips in the control group (untreated) were infected with *Penicillium oryzae* (PC), *Trichoderma viride* (TV), *Aspergillus niger* (AN), and a mix of the three molds (PTA), and their surfaces were mostly covered with mold. Among them, the bamboo strips infected with AN and PTA were severely discolored and mostly appeared black, showing that the untreated bamboo had no antifungal properties. In contrast, the surface of the bamboo strips treated with the composite hydrogel were rarely infected by PC, TV, AN, or PTA. Reasonable explanations for this are as follows: First, AgNPs loaded on NIPAm polymer carrier could be continuously released due to the temperature-sensitive properties of the polymer, so that the system maintained a relatively constant silver concentration; Secondly, AgNPs itself has spectral antibacterial properties, and can synergistic release Ag^+ to play an antibacterial role; Finally, and more importantly, the synergistic effect of PVP and AAc can better achieve the decentralized protection effect, effectively inhibiting the aggregation and deposition of AgNPs and avoiding oxidation. Figures 7a and 7b show the strips treated with the NIPAm/AAc/AgNPs composite hydrogels mostly maintained their original color. This is consistent with the idea that the addition of PVP and AAc inhibits the oxidation blackening of silver. To sum up, the composite hydrogel displayed excellent anti-mold properties against common bamboo molds.



(a)



(b)



(c)

Notes: *Penicillium citrinum* (PC), *Trichoderma viride* (TV), *Aspergillus niger* (AN), and mixed molds (PC, TV, and AN in a 1 to 1 to 1 ratio, abbreviated as PTA), A or orange represents the untreated group (control), B or green represents the treated group (sample).

Fig. 7. (a) Anti-mold results of bamboo strips treated with the composite hydrogels; (b) Mouldproof level of the bamboo strips treated with the composite hydrogels; (c) Anti-mold results of the PTA treated with the silver-loaded thermo-sensitive nanogel bamboo strips (Yu *et al.* 2017)

CONCLUSIONS

1. Poly(N-isopropyl acrylamide) (NIPAm) and acrylic acid (AAc) were used as hydrogel matrix, AgNO_3 was used as silver source, polyvinyl pyrrolidone (PVP) was used as protective agent, and NIPAm/AAc/AgNPs composite hydrogel was successfully prepared by free radical polymerization. When the AAc concentration was $0.64 \mu\text{L/mL}$, the hydrogel produced displayed the smallest particle size (59.4 nm) and the best dispersion.
2. After the treatment of the composite hydrogel, the bamboo intercellular space, cell lumens, and cell walls were filled with the composite hydrogel and AgNPs particles, and the parenchyma cells and ducts of the bamboo material still maintained the original microstructure.
3. The anti-mold experiment results showed that the composite hydrogel demonstrated

an enormous anti-mold effect for *Penicillium oryzae* (PC), *Trichoderma viride* (TV), *Aspergillus niger* (AN) as well as for the mixed mold (PTA), which are all commonly found on bamboo.

4. The bamboo strips used in the anti-mold test mostly maintained their original color.

ACKNOWLEDGMENTS

The authors appreciate the financial support from the National Natural Science Foundation of China (Grant no. 31870541 and 31370568).

REFERENCES CITED

- Begum, R., Naseem, K., Ahmed, E., Sharif, A., and Farooqi, Z. H. (2016). "Simultaneous catalytic reduction of nitroarenes using silver nanoparticles fabricated in poly(*N*-isopropylacrylamide-acrylic acid-acrylamide) microgels," *Colloids and Surfaces A: Physicochemical and Engineering Aspects* 511, 17-26. DOI: 10.1016/j.colsurfa.2016.09.076
- Chung, K. F., and Yu, W. K. (2002). "Mechanical properties of structural bamboo for bamboo scaffoldings," *Engineering Structures* 24(4), 429-442. DOI: 10.1016/S0141-0296(01)00110-9
- Devaki, S. J., Narayanan, R. K., and Sarojam, S. (2014). "Electrically conducting silver nanoparticle-polyacrylic acid hydrogel by in situ reduction and polymerization approach," *Materials Letters* 116, 135-138. DOI: 10.1016/j.matlet.2013.10.110
- Eghbalifam, N., Frounchi, M., and Dadbin, S. (2015). "Antibacterial silver nanoparticles in polyvinyl alcohol/sodium alginate blend produced by gamma irradiation," *International Journal of Biological Macromolecules* 80, 170-176. DOI: 10.1016/j.ijbiomac.2015.06.042
- Gao, C., An, Q., Xiao, Z., Zhai, S., Zhai, B., and Shi, Z. (2018). "Alginate and polyethyleneimine dually mediated synthesis of nanosilver-containing composites for efficient p-nitrophenol reduction," *Carbohydrate Polymers* 181, 744-751. DOI: 10.1016/j.carbpol.2017.11.083
- GB/T18261 (2013). "Test method for the effectiveness of antimold agents against wood molds and discoloration fungi," Standardization Administration of China, Beijing, China.
- Ge, Y., Duan, X., Zhang, M., Mei, L., Hu, J., Hu, W., and Duan, X. (2017). "Direct room temperature welding and chemical protection of silver nanowire thin films for high performance transparent conductors," *Journal of the American Chemical Society* 140(1), 193-199. DOI: 10.1021/jacs.7b07851
- Gilcrease, E. B., Williams, R., and Goel, R. (2020). "Evaluating the effect of silver nanoparticles on bacteriophage lytic infection cycle-a mechanistic understanding," *Water Research* 181, 115900. DOI: 10.1016/j.watres.2020.115900
- Guo, W., Lu, C.-H., Qi, X.-J., Orbach, R., Fadeev, M., Yang, H.-H., and Willner, I. (2014). "Switchable bifunctional stimuli-triggered poly-*N*-isopropylacrylamide/DNA hydrogels," *Angewandte Chemie International Edition* 53(38), 10134-10138. DOI: 10.1002/anie.201405692

- He, M., Wang, Q., Wang, R., Xie, Y., Zhao, W., and Zhao, C. (2017a). "Design of antibacterial poly(ether sulfone) membranes via covalently attaching hydrogel thin layers loaded with Ag nanoparticles," *ACS Applied Materials & Interfaces* 9(19). DOI: 10.1021/acsami.7b03176
- He, M., Wang, Q., Zhang, J., Zhao, W., and Zhao, C. (2017b). "Substrate independent Ag nanoparticles loaded hydrogel coating with regenerable bactericidal and thermo-responsive anti-bacterial properties," *ACS Applied Materials & Interfaces* 9(51), 44782-44791. DOI: 10.1021/acsami.7b13238
- Hong, X., Zhang, B., Murphy, E., Zou, J., and Kim, F. (2017). "Three-dimensional reduced graphene oxide/polyaniline nanocomposite film prepared by diffusion driven layer-by-layer assembly for high-performance supercapacitors," *Journal of Power Sources* 343, 60-66. DOI: 10.1016/j.jpowsour.2017.01.034
- Hu, H., Liu, M., Kong, Y., Mysuru, N., Sun, C., Gálvez-Vázquez, M. d. J., Müller, U., Erni, R., Grozovski, V., Hou, Y., *et al.* (2020). "Activation matters: Hysteresis effects during electrochemical looping of colloidal Ag nanowire (Ag-NW) catalysts," *ACS Catalysis* 10(15), 8503-8514. DOI: 10.1021/acscatal.0c02026
- Hu, H., Xin, J. H., and Hu, H. (2014). "PAM/graphene/Ag ternary hydrogel: Synthesis, characterization and catalytic application," *Journal of Materials Chemistry A* 2(29), 11319-11333. DOI: 10.1039/c4ta01620c
- Huang, Q., Du, C., Hua, Y., Zhang, J., Peng, R., and Yao, X. (2019). "Synthesis and characterization of loaded nano/zinc oxide composite hydrogels intended for anti-mold coatings on bamboo," *BioResources* 14(3), 7134-7147. DOI: 10.15376/biores.14.3.7134-7147
- Liu, G., Lu, Z., Zhu, X., Du, X., Hu, J., Chang, S., Li, X., and Liu, Y. (2019). "Facile *in situ* growth of Ag/TiO₂ nanoparticles on polydopamine modified bamboo with excellent mildew-proofing," *Scientific Reports* 9(1), 16496. DOI: 10.1038/s41598-019-53001-y
- Liu, T., Zhang, W., Wang, J., Zhang, Y., Wang, H., Sun, and F., Cai, L. (2020). "Improved dimensional stability and mold resistance of bamboo via *in situ* growth of poly(hydroxyethyl methacrylate-*N*-Isopropyl acrylamide)," *Polymers* 12(7), 1584-1597. DOI: 10.3390/polym12071584
- Ma, Y., Shi, L., Liu, F., Zhang, Y., Pang, Y., and Shen, X. (2019). "Self-assembled thixotropic silver cluster hydrogel for anticancer drug release," *Chemical Engineering Journal* 362, 650-657. DOI: 10.1016/j.cej.2019.01.096
- Meng, M., He, H., Xiao, J., Zhao, P., Xie, J., and Lu, Z. (2016). "Controllable *in situ* synthesis of silver nanoparticles on multilayered film-coated silk fibers for antibacterial application," *Journal of Colloid and Interface Science* 461, 369-375. DOI: 10.1016/j.jcis.2015.09.038
- Qi, X., Balankura, T., and Fichthorn, K. A. (2018). "Theoretical perspectives on the influence of solution-phase additives in shape-controlled nanocrystal synthesis," *The Journal of Physical Chemistry C* 122(33), 18785-18794. DOI: 10.1021/acs.jpcc.8b00562
- Sharma, B., Gatóo, A., Bock, M., and Ramage, M. (2015). "Engineered bamboo for structural applications," *Construction and Building Materials* 81, 66-73. DOI: 10.1016/j.conbuildmat.2015.01.077
- Shi, Q. S., and Li, W. R. (2018). "Comparative analysis of anti-bacterial properties and anti-bacterial kinetics between silver ions and nano-silver," in: *Proceedings of the 3rd Antibacterial Science and Technology Forum*, Beijing, China, pp. 45-46.

- Taylor, P. L., Ussher, A. L., and Burrell, R. E. (2005). "Impact of heat on nanocrystalline silver dressings: Part I: Chemical and biological properties," *Biomaterials* 26(35), 7221-7229. DOI: 10.1016/j.biomaterials.2005.05.040
- Wang, J., Pan, X., and Wang, S. (2016). "Preparation and characterization of polyglutamic/chitosan/nano-silver composite hydrogels." *Ion Exchange and Adsorption* 32(4), 297-305.
- Wei, J., Chen, Y., Liu, H., Du, C., Yu, H., and Zhou, Z. (2016). "Thermo-responsive and compression properties of TEMPO-oxidized cellulose nanofiber-modified PNIPAm hydrogels," *Carbohydrate Polymers* 147, 201-207. DOI: 10.1016/j.carbpol.2016.04.015
- Wei, J., Yu, H., Liu, H., Du, C., Zhou, Z., Huang, Q., and Yao, X. (2018). "Facile synthesis of thermo-responsive nanogels less than 50 nm in diameter via soap- and heat-free precipitation polymerization," *Journal of Materials Science* 53(17), 12056-12064. DOI: 10.1007/s10853-018-2495-x
- Wu, W., Zhou, T., Berliner, A., Banerjee, P., and Zhou, S. (2010). "Smart core-shell hybrid nanogels with Ag nanoparticle core for cancer cell imaging and gel shell for pH-regulated drug delivery," *Chemistry of Materials* 22(6), 1966-1976. DOI: 10.1021/cm903357q
- Wu, Z., Huang, D., Wei, W., Wang, W., Wang, X., Wei, Q., Niu, M., Lin, M., Rao, J., and Xie, Y. (2019). "Mesoporous aluminosilicate improves mildew resistance of bamboo scrimber with Cu-B-P anti-mildew agents," *Journal of Cleaner Production* 209, 273-282. DOI: 10.1016/j.jclepro.2018.10.168
- Yu, H., Du, C., Liu, H., Wei, J., Zhou, Z., Huang, Q., and Yao, X. (2017). "Preparation and characterization of bamboo strips impregnation treated by silver-loaded thermo-sensitive nanogels," *BioResources* 12(4), 8390-8401. DOI: 10.15376/biores.12.4.8390-8401
- Yuan, Z., Wen, Y., Kapu, N. S., Beatson, R., and Martinez, D. M. (2017). "A biorefinery scheme to fractionate bamboo into high-grade dissolving pulp and ethanol," *Biotechnology for Biofuels* 10(38), 1-16. DOI: 10.1186/s13068-017-0723-2
- Zhang, J., Huang, Q., Du, C., Peng, R., Hua, Y., Li, Q., Hu, A., and Zhou, J. (2020). "Preparation and anti-mold properties of nano-ZnO/poly(*N*-isopropylacrylamide) composite hydrogels," *Molecules* 25(18), 4135-4145. DOI: 10.3390/molecules25184135
- Zhou, H., Xu, H., and Liu, Y. (2019). "Aerobic oxidation of 5-hydroxymethylfurfural to 2,5-furandicarboxylic acid over Co/Mn-lignin coordination complexes-derived catalysts," *Applied Catalysis B: Environmental* 244, 965-973. DOI: 10.1016/j.apcatb.2018.12.046

Article submitted: October 20, 2020; Peer review completed: November 15, 2020;
Revised version received and accepted: November 18, 2020; Published: November 20, 2020.

DOI: 10.15376/biores.16.1.441-454